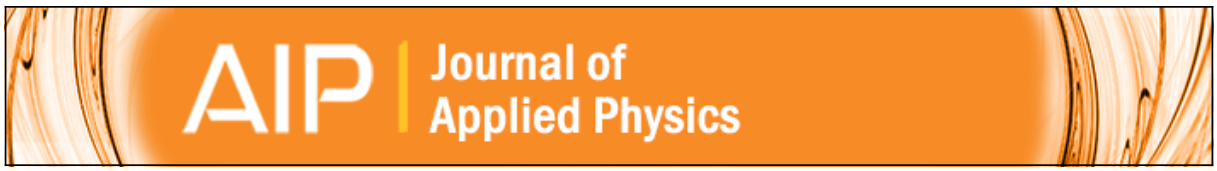


# Wavelength and composition dependence of the thermo-optic coefficient for InGaAsP-based integrated waveguides

Daniele Melati, Abi Waqas, Andrea Alippi, and Andrea Melloni

Citation: Journal of Applied Physics **120**, 213102 (2016); doi: 10.1063/1.4970937

View online: http://dx.doi.org/10.1063/1.4970937

View Table of Contents: http://scitation.aip.org/content/aip/journal/jap/120/21?ver=pdfcov

Published by the AIP Publishing



JOURNAL OF APPLIED PHYSICS **120**, 213102 (2016)

# Wavelength and composition dependence of the thermo-optic coefficient for InGaAsP-based integrated waveguides

Daniele Melati,[a] Abi Waqas, Andrea Alippi,[b] and Andrea Melloni
*Dipartimento di Elettronica, Informazione e Bioingegneria, Politecnico di Milano, 20133 Milano, Italy*

(Received 1 July 2016; accepted 16 November 2016; published online 2 December 2016)

A method to take into account the wavelength, composition, and temperature dependencies in the calculation of the refractive index and linear thermo-optic coefficient of $In_{1-x}Ga_xAs_yP_{1-y}$ alloys is presented. The method, based on the modified single oscillator model, shows a good agreement with experimental data for InP reported in literature at different wavelength and temperature ranges. Further, we exploit this approach with a Film-Mode Matching solver to calculate the linear thermo-optic coefficients of both phase and group effective indices of an InGaAsP-based waveguide. The same waveguide structure is also experimentally investigated through a reflectometric technique and results are found to be in accordance with the simulations performed exploiting the proposed method. In both cases, a dependence of the group index on temperature, almost twice that of the phase index, is observed. These results provide a deeper understanding on the influence of the temperature on the behaviour of optical waveguides and devices, making possible an accurate and realistic modelling of integrated circuits. *Published by AIP Publishing.*
[http://dx.doi.org/10.1063/1.4970937]

## I. INTRODUCTION

Thermal handling is one of the fundamental issues in the effective exploitation of integrated photonic circuits. Unavoidable temperature gradients and fluctuations can significantly alter the behaviour of many devices. Likewise, thermal cross-talk (where heat generated by a device affects the temperature of nearby structures) can lead to undesired spurious effects.[1] Hence, the precise measurement and modelling of the thermo-optic properties of the materials is fundamental to correctly predict these phenomena during the design of both devices and complex circuits.

Among other technologies, InP/InGaAsP-based platforms are nowadays the elective choice for the monolithic integration of passive and active photonic devices. Waveguides generally exploit binary InP as substrate and InGaAsP for the core, eventually through Multiple-Quantum well structures.[2] The InGaAsP quaternary alloy can be grown over an extensive range of compositions while respecting lattice matching with InP, and the resulting energy bandgap varies from about 1.35 eV (0.92 $\mu$m) to about 0.75 eV (1.65$\mu$m).[3,4] The most recurring approaches considered in literature for the estimation of the wavelength- and composition-dependent refractive index of InGaAsP and related binary and ternary alloys include the empirical Sellmeier equation, the single oscillator model, the modified single oscillator model (MSOM) and the Adachi model.[5,6] All of them, in their basic formulation, do not directly include temperature dependence and may hence become imprecise far from room temperature.[7] One solution has been proposed by Weber through an extension of the model given by Adachi[5] but predicted results are considerably different from many experimental data reported in literature.[8–10] For different binary and ternary III-V compounds (e.g., AlGaAs) Kim and Sarangan formulated an extension of the Sellmeier equation that results to be in good agreement with measured data.[7] For InP, Gini,[10] and Martin[9] proposed a least square fit model to calculate the wavelength dependence of the thermo-optic coefficient based on experimental data.

The aim of this work is to model and experimentally verify the thermo-optic coefficient dn/dT and its dependence on wavelength and material composition for InGaAsP compounds. To this purpose, we propose to include temperature dependence in the calculation of the refractive index of $In_{1-x}Ga_xAs_yP_{1-y}$ alloys through the modified single oscillator model. This approach allows to calculate the wavelength, composition, and temperature dependence of the refractive index of the material, and hence, of the linear thermo-optic coefficient, providing a very good agreement with data available in literature.[8,10] The proposed approach is used in combination with a Film-Mode Matching mode solver[11] to calculate the linear thermo-optic coefficient of both phase and group effective indices of an InGaAsP-based waveguide, and results are found to be in accordance with the experimental characterizations performed by means of the reflectometric technique described in Ref. 12. Both model and measurements reveal that the dependence of the effective group index of the waveguides to temperature is almost twice that of the effective phase index.

The paper is organized as follows. Section II presents the background review of the modified single oscillator model. In Section III, the proposed extension for temperature dependence is presented and the numerical results are compared with other existing models and experimental data available in literature for InP. Section IV describes the exploited measurement technique and reports the characterization of the thermo-optic coefficients of both phase and group effective indices, compared with the results

[a]daniele.melati@polimi.it.
[b]Present address: Linkra Microtech, 20864 Agrate Brianza, Italy.

obtained through modal simulations exploiting the proposed method.

## II. BACKGROUND REVIEW: MODIFIED SINGLE OSCILLATOR MODEL

The modified single oscillator model (MSOM)[13] is a semi-empirical method for the estimation of the room temperature refractive index for a large class of III-V semiconductors commonly used in literature.[13,14] Focusing on InP-based alloys, the refractive index of the $In_{1-x}Ga_xAs_yP_{1-y}$ crystal at a given optical frequency $\nu$ can be found through the relation

$$n^2 = 1 + \frac{E_d}{E_o} + \frac{E_d}{E_o^3}E^2 + \frac{\eta}{\pi}E^4 \ln\left(\frac{2E_o - E_g^2 - E^2}{E_g^2 - E^2}\right), \quad (1)$$

where

$$\eta = \frac{\pi E_d}{2E_o^3\left(E_o^2 - E_g^2\right)}. \quad (2)$$

In Equations (1) and (2), $E = h\nu$ is the photon energy; $E_o$ is the energy of the single-effective oscillator in the intrinsic absorption region (where imaginary part of complex dielectric constant reaches to maximum); $E_d$ is the dispersion energy, related to the strength of interband optical transitions; $E_g = hc/\lambda_g$ is the bandgap energy, $\lambda_g$ being the bandgap wavelength. The relation $y = 2.197x$[13,15] between the gallium concentration $x$ and the arsenic concentration $y$ in the quaternary alloy is valid assuming the lattice matching with InP (a fundamental requirement for the fabrication of InGaAsP-based waveguides). The characteristic parameters $E_o$, $E_d$, and $E_g$ are hence derived from the experimental data of InGaP and InGaAs at room temperature (300 K) with an interpolation method[13] and are related to the amount of arsenic $y$ by the empirical relations[13,14]

$$E_o(y) = 3.391 - 1.652y + 0.863y^2 - 0.123y^3, \quad (3a)$$

$$E_d(y) = 28.91 - 9.278y + 5.626y^2, \quad (3b)$$

$$E_g(y) = 1.35 - 0.72y + 0.12y^2. \quad (3c)$$

As can be clearly seen, the modified single oscillator model used in literature does not explicitly include a temperature-dependence for $E_o$, $E_d$, and $E_g$, and consequently, for the refractive index $n$.

## III. TEMPERATURE DEPENDENCE OF THE REFRACTIVE INDEX OF InGaAsP COMPOUNDS

### A. Proposed method

In order to take into account the temperature dependence, along with wavelength and composition dependence, in the calculation of the refractive index for $In_{1-x}Ga_xAs_yP_{1-y}$ alloys through the modified single oscillator model, it is necessary to evaluate the effect of the temperature on the three parameters $E_g$, $E_d$, and $E_o$. To this purpose, we exploit the equation proposed by Varshni in Ref. 16. This widely exploited model allows to predict the dependence of the energy bandgap $E_g$ with temperature in semiconductors and can be expressed in the form

$$E_g(T) = E_{go} - \frac{\alpha T^2}{T + \beta}, \quad (4)$$

where $E_{go}$ is the energy bandgap value at the temperature of 0 K, T is the temperature in Kelvin degrees, and $\alpha$ and $\beta$ are two fitting constants.

Interestingly, Nakajima[3] and Fiedler[14] observed that the energy bandgap $E_g$ of the quaternary allow $In_{1-x}Ga_xAs_yP_{1-y}$ at a given temperature is linearly dependent on the composition parameters $x$ and $y$. As reviewed in Sec. II, for $In_{1-x}Ga_xAs_yP_{1-y}$, $E_g$ at 300 K can be expressed as a function of the composition through Equation (3c). At 0 K the same relation becomes $E_g = 1.421 - 0.72y + 0.12y^2$, as reported in Refs. 3 and 14. In these two equations, 1.35 eV and 1.421 eV represent the energy bandgap of InP at temperatures of 300 K and 0 K, respectively. It can also be observed that the coefficients related to the composition variable $y$ are unaffected by temperature variations. Taking this into account and substituting Equation (4) in Equation (3c), the energy bandgap can be calculated as function of temperature and composition as

$$E_g(T, y) = \left(1.421 - \frac{\alpha T^2}{T + \beta}\right) - 0.72y + 0.12y^2. \quad (5)$$

The constants $\alpha$ and $\beta$ can be obtained by fitting the values of the energy bandgap of InP at 0 K and 300 K reported above, resulting in $\alpha = 7.2 \times 10^{-4}$ and $\beta = 611$. The same values for these two fitting constants are reported also in Ref. 4.

To estimate the temperature dependence of the other two characteristic parameters $E_o$ and $E_d$, we propose to convert the effects of temperature variations in an equivalent variation of the arsenic concentration at room temperature. First, for the desired concentration of the arsenic $y$ and temperature $T$, we calculate the corresponding energy bandgap $E_g(T, y)$ through Equation (5). Hence, we exploit Equation (3c) to obtain the equivalent arsenic concentration

$$\tilde{y} = 3.0 - \sqrt{8.33E_g(T, y) - 2.25}, \quad (6)$$

where $\tilde{y}$ represents the arsenic concentration that would provide, at room temperature, the same energy bandgap we calculated at temperature $T$ with Equation (5). We finally use $\tilde{y}$ in Equations (3a) and (3b) to calculate the remaining parameters $E_o$ and $E_d$. Figure 1 reports the values obtained for the three characteristic parameters for all the possible arsenic concentrations ($y$ from 0 to 1) and temperature ranging from 0 K to 500 K.

The described approach takes into account the temperature dependence in the calculation of the refractive index of $In_{1-x}Ga_xAs_yP_{1-y}$ compounds with arbitrary composition through the modified single oscillator model (1), and hence, allows to predict the wavelength dependence of the thermo-optic coefficient for these alloys. At room temperature, the results obtained with this method are identical to those generated by Equations (3a)–(3c) by definition.

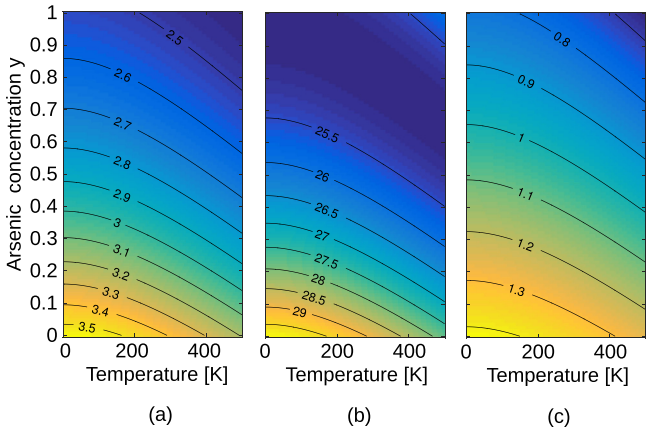


FIG. 1. Values of (a) $E_o$, (b) $E_d$, and (c) $E_g$ obtained with the proposed method as function of temperature and arsenic concentration $y$.

### B. Linear approximation

A simpler approach that can be used to estimate the effects of temperature variations on $E_o$ and $E_d$ is based on the empirical linear relation between $E_o$, $E_d$, and $E_g$ suggested by Takagi[17,18] and Afromowitz.[19] In particular, it is possible to linearly approximate the characteristic parameters $E_o$ and $E_d$ for InGaAsP by fitting Equations (3a)–(3c), resulting in

$$E_o(T,y) = 1.894E_g(T,y) + 0.8116, \tag{7}$$

$$E_d(T,y) = 9.835E_g(T,y) + 15.455. \tag{8}$$

The linear approximation obtained in Equations (7) and (8) is the same as reported in Ref. 18 at room temperature. Calculating $E_g(T,y)$ through Equation (5) and assuming the coefficients of the fitting to be temperature-independent, Equations (7) and (8) allow to calculate the temperature dependence for $E_o$ and $E_d$.

To check the consistency of Equations (7) and (8) with the original MSOM Equations (3a) and (3b) at room temperature, Fig. 2 reports the comparison between the results obtained with the two approaches for both the oscillation energy $E_o$ and the dispersion energy $E_d$. As can be seen, in both cases the linear approximation holds for $E_g$ larger than of about 1.0 eV, corresponding to $y < 0.5$. Out of this range, the linear approximation becomes significantly less accurate.

### C. Numerical results and comparison with existing models

In order to verify the proposed method, this section compares the calculated refractive index $n$ at room temperature $T = 300\,K$ and wavelength $\lambda = 1.55\,\mu m$ for a different mole fraction $y$ of arsenic with the values obtained through other well established models. The comparison is shown in Fig. 3. The refractive index calculated exploiting the proposed method described in Section III A and Equation (1) is shown with solid line. For comparison, the figure also reports the results obtained with Equations (7) and (8) (linear approximation, dashed line), with the Weber's extension of the Adachi model[5,6] (stars) and with the Sellmeier equation[14]

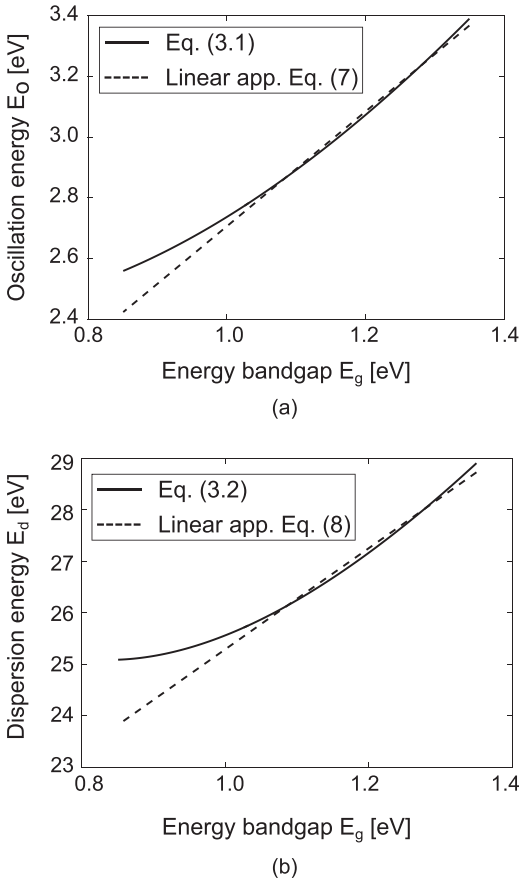


FIG. 2. (a) Oscillation energy $E_o$ and (b) dispersion energy $E_d$ as function of the energy bandgap $E_g$ from modified single oscillator model (solid line) and linear approximation (dashed line) at room temperature.

(dotted line). The arsenic concentration $y$ ranges from 0 (corresponding to binary InP) to 0.8.

As can be seen, at room temperature all the models are in very good agreement for $y < 0.5$, excluding the Sellmeier equation that predicts a significantly different behaviour (the refractive index difference with respect to the other models

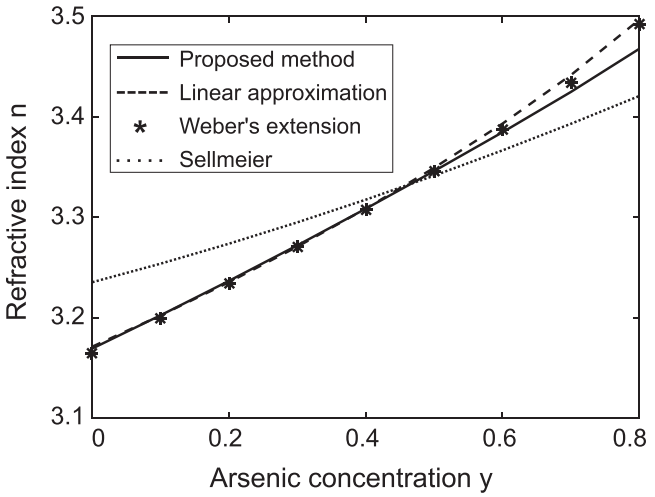


FIG. 3. Estimation of the refractive index for InGaAsP as function of the arsenic concentration $y$ at wavelength $\lambda = 1.55\,\mu m$ and temperature $T = 300\,K$ obtained with the proposed method and with other models available in literature.

is about 0.07 for $y = 0$). The refractive index predicted by the other considered models starts to diverge for $y > 0.5$. As already mentioned, the proposed method is equivalent to MSOM, since the results refer to room temperature. It can be noticed that, as expected, the use of the linear approximation in Equations (7) and (8) causes a significant deviation of the predicted refractive index compared MSOM for $y > 0.5$, consistently with the results reported in Fig. 2. The results obtained through the Weber's extension of the Adachi model match the linear approximation.

The proposed method, the linear approximation and the Weber's extension allow to investigate also the dependence of the refractive index on temperature. Results are shown in Fig. 4 that reports the calculated refractive index as function of the temperature from $T = 250\,K$ to $T = 450\,K$, for three different values of arsenic concentration ($y = 0$, $y = 0.26$, and $y = 0.7$) at wavelength $\lambda = 1.55$ $\mu$m. All the models predict an almost linear dependence of the refractive index on temperature. This linear relation has also been experimentally confirmed by several works for binary (InP, GaAs),[10,20] ternary ($Al_xGa_{1-x}As$, for $x$ changing from 0 to 1)[7] and quaternary alloys ($In_{1-x}Ga_xAs_yP_{1-y}$, at least for $y = 0.32$ and $y = 0.6$).[21] As can be seen in Fig. 4, the proposed method predicts a larger thermal dependence of the refractive index for InP compared to the Weber's extension (at room temperature, $dn/dT = 1.93 \times 10^{-4}$ instead of $dn/dT = 1.13 \times 10^{-4}$). The same is true for InGaAsP, with an even larger difference ($dn/dT = 2.28 \times 10^{-4}$ for the proposed method and $dn/dT = 1.26 \times 10^{-4}$ for the Weber's extension with $y = 0.26$). As expected, the linear approximation is in perfect agreement with the proposed method only for $y < 0.5$.

### D. Thermo-optic coefficient

The thermo-optic coefficient of the materials can be obtained by the temperature dependence of the refractive index predicted by the various considered models. As for the previous results, the proposed method, the linear approximation, and the Weber's extension of the Adachi model are taken into account and the results are reported in Fig. 5.

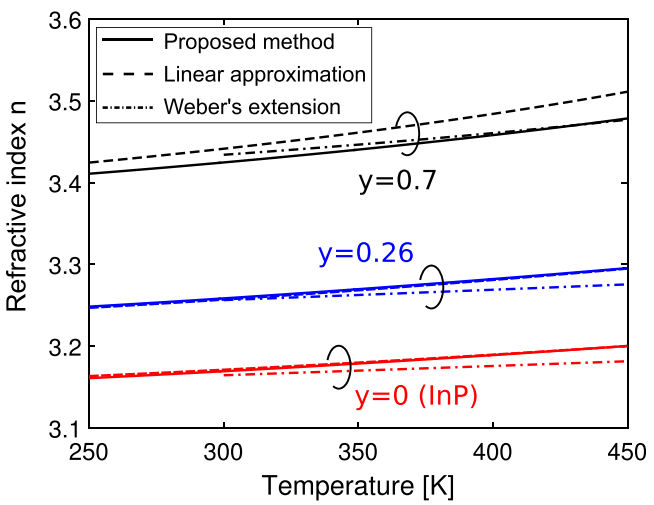


FIG. 4. Dependence of the refractive index with temperature at wavelength $\lambda = 1.55$ $\mu$m with $y = 0$ (red), $y = 0.26$ (blue), and $y = 0.7$ (black).

Figure 5(a) shows the predicted dependence of the thermo-optic coefficient dn/dT on wavelength at room temperature for $y = 0$, $y = 0.26$, and $y = 0.7$. Wavelength ranges from $\lambda = 1.2$ $\mu$m to $\lambda = 1.6$ $\mu$m except for $y = 0.7$ because of the bandgap $\lambda_g = 1.37$ $\mu$m at $T = 300\,K$. The experimental data reported in Refs. 8–10 for InP are shown with circle and cross markers. As can be seen, in their work Gini *et al.* (crosses) observed a variation of the thermo-optic coefficient for InP from $2.30 \times 10^{-4}$ to $1.90 \times 10^{-4}$ in the considered wavelength range. These data are consistent with those reported by Della Corte *et al.* and Martin *et al.* (circle) for $\lambda = 1.5$ $\mu$m and $T = 300\,K$. The results obtained with the proposed method (solid line) are in very good agreement with these data, with a maximum difference between prediction and experimental data in the order of $10^{-6}$ from $\lambda = 1.2$ $\mu$m to $\lambda = 1.55$ $\mu$m. The difference is slightly higher ($10^{-5}$) at

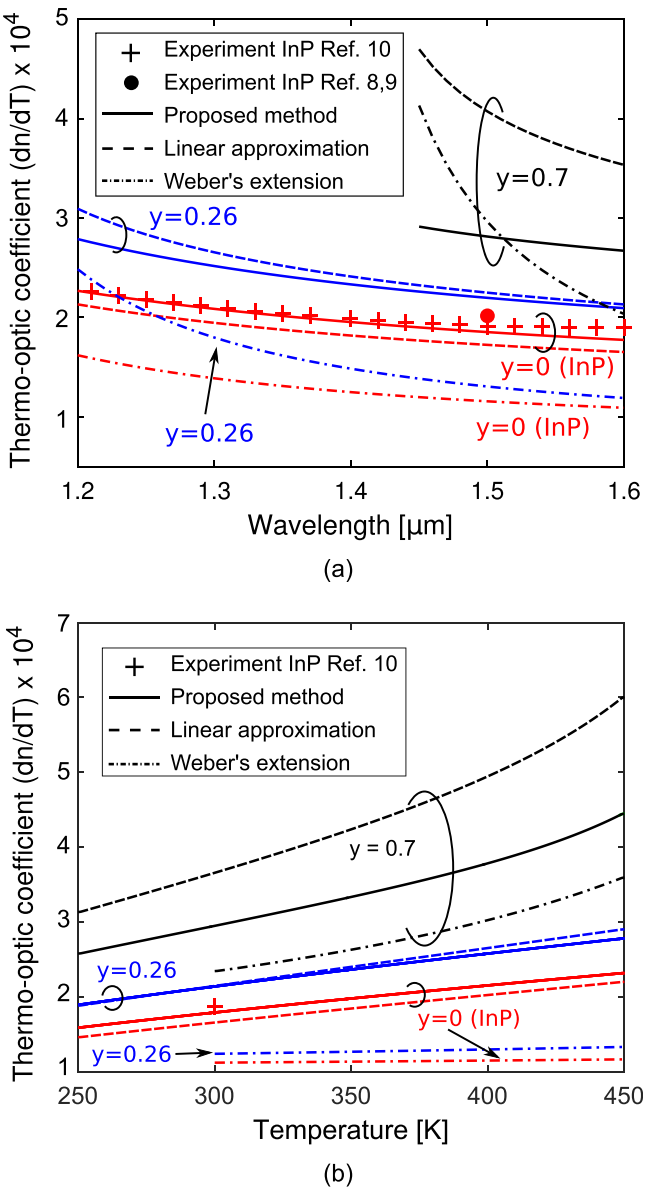


FIG. 5. Dependence of the thermo-optic coefficient with (a) wavelength (for fixed temperature $T = 300\,K$) and (b) temperature (for fixed wavelength $\lambda = 1.55$ $\mu$m) for $y = 0$ (red), $y = 0.26$ (blue), and $y = 0.7$ (black). Experimental data reported in Ref. 8–10 for InP are also shown with circle and cross markers.

$\lambda = 1.6$ $\mu$m. The predictions of the Weber's extension for the wavelength-dependent thermo-optic coefficients of InP (dot-dashed line) are rather different from the experimental data, with dn/dT ranging from $1.63 \times 10^{-4}$ to $1.09 \cdot 10^{-4}$ in the considered wavelength range. Also for InGaAsP with $y = 0.26$, the results for the two methods are considerably different, with variations between $2.80 \times 10^{-4}$ and $2.10 \times 10^{-4}$ for the proposed approach and $2.48 \times 10^{-4}$ to $1.20 \times 10^{-4}$ for the Weber's extension. For $y = 0.7$ the difference is even larger, especially for $\lambda > 1.5$ $\mu$m, with different predictions of the value of the thermo-optic coefficient ($2.74 \times 10^{-4}$ for the proposed method and $2.39 \times 10^{-4}$ for the Weber's extension at $\lambda = 1.55$ $\mu$m) as well as its dependence on wavelength. As expected, the results obtained with the linear approximation are closer to those obtained with the proposed method for both $y = 0$ and $y = 0.26$, while at $y = 0.7$ the difference grows up to $1.78 \times 10^{-4}$ for wavelengths closer to the bandgap. At $\lambda = 1.55$ $\mu$m the difference is about $1.01 \times 10^{-4}$.

Similar results were obtained by investigating the dependence of the thermo-optic coefficient on temperature from T = 250 K to T = 450 K, as reported in Fig. 5(b) for $\lambda = 1.55$ $\mu$m. The experimental result reported in Ref. 10 for InP at $\lambda = 1.55$ $\mu$m and T = 300 K is shown again for reference. Consistently, the Weber's extension predicts a smaller thermo-optic coefficient and also a weaker dependence on temperature compared to the proposed method (for $y = 0$ and $y = 0.26$ Weber's extension suggests a coefficient almost independent on temperature). The latter shows a similar variation of about $8 \times 10^{-5}$ in the coefficient in a temperature range of 200 K for both $y = 0$ and $y = 0.26$. The dependence is stronger for $y = 0.7$ and $T > 400$ K because of the closer bandgap. The results of the linear approximation are again in good agreement with the proposed method only for $y < 0.5$.

Last, the results obtained with the proposed method are compared with experimental values of the thermo-optic coefficient available in literature for InP ($y = 0$). The comparison is reported in Table I, where two temperature and wavelength ranges are taken into account. As can be seen, in all the cases the predictions are in good agreement with the experimental data. The first line (Ref. 10) corresponds to the data reported in Fig. 5 with red crosses and as already noticed the maximum discrepancy between experimental data and model prediction is less than $10^{-5}$. A similar accuracy is obtained for $\lambda = 1.5$ $\mu$m and temperature ranging from 300 K to 600 K (Refs. 8 and 9, reported in Fig. 5(a) with red circle for $\lambda = 1.5\mu$m and T = 300 K). A similar comparison is also reported in the Appendix, where the proposed method is applied to a different III-V binary compound (GaAs).

TABLE I. Comparison between the thermo-optic coefficient predicted through the proposed approach and data reported in literature for InP in different temperature and wavelength ranges.

| Temperature/wavelength | Data from literature | This work |
|---|---|---|
| 283–333 K, 1.2–1.6 $\mu$m | 2.27–1.90 $\times 10^{-4}$ (Ref. 10) | 2.30–1.81 $\times 10^{-4}$ |
| 300–600 K, 1.5 $\mu$m | 2.0–2.40 $\times 10^{-4}$ (Refs. 8 and 9) | 1.85–2.37 $\times 10^{-4}$ |

## IV. EXPERIMENTAL RESULTS ON INTEGRATED WAVEGUIDES

In this section, we present an application of the described method (combined with a Film-Mode Matching mode solver[11]) for the estimation of the wavelength-dependent thermo-optic coefficient of InGaAsP-based waveguides and compare the results with experimental characterizations. Wavelength dependence is expressed in terms of thermo-optic coefficients for both phase and group effective indices in a wavelength range of 60 nm to around 1550 nm and a temperature range of 20 K to around 300 K.

### A. Measurement technique

The reflectometric technique used in this work for the experimental characterization of the thermal properties of InGaAsP-based waveguides exploits the Point Reflector Optical Waveguide (PROW) structures proposed in Ref. 12 for multi-point on-wafer optical testing. A PROW consists of an integrated waveguide carrying multiple sensing probes based on lumped reflectors that can be used to locally measure the optical parameters of the waveguide. The PROW interrogation scheme is based on the Optical Frequency-Domain Reflectometry (OFDR) technique.[22,23] Through the measurement of the optical spectrum of the light back-reflected by the PROW, OFDR allows to retrieve the spatial distribution of the reflective sections in the structure contributing to the total reflected power, providing their complex reflection coefficient (amplitude and phase). From this measurement it is possible to estimate the local value of the phase and group indices with a single experimental data acquisition. A detailed description of the estimation technique for phase and group indices by means of the PROW structure can be found in Ref. 12. We report here the fundamental concepts relevant for the reported investigation.

The sketch of a PROW can be seen in Fig. 6(a), showing a single-mode waveguide with several reflective elements. By means of a first-order Taylor expansion, it is possible to write the phase associated to the light reflected by one of the reflective elements A around the central frequency $\omega_0$ as

$$\varphi_A(\omega) + 2N\pi = \beta(\omega)L_A = \beta_0 L_A + \beta_1 L_A(\omega - \omega_0), \quad (9)$$

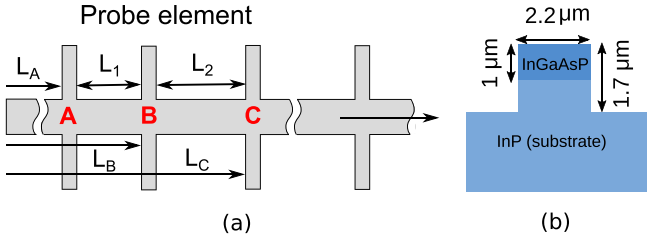


FIG. 6. (a) Sketch of the PROW exploited to measure the optical parameters of the waveguide. Each sensing point is made by three reflective sections. (b) Cross-section of the measured waveguide.

where $L_A$ is the distance between the input of the waveguide and the reflector A, $\beta_0 = \omega_0/cn_{\text{eff}}$, $\beta_1 = c/n_g$, N is the integer number of $2\pi$ accumulated during propagation and the phase $\varphi_A$ is defined between $-\pi$ and $+\pi$. A single probe element in the PROW is made by three reflectors spaced by two waveguide sections of length $L_1$ and $L_2$, respectively. The technique assumes all the optical properties of the waveguide being constant over the probe length, which acts as a unitary sensing element. Starting from the absolute phases associated to the three reflective sections ($\varphi_A$, $\varphi_B$, $\varphi_C$) of a probe element, we can define the phase difference as

$$\begin{aligned}\Delta\varphi(\omega) &= \varphi_C(\omega) - 2\varphi_B(\omega) - \varphi_A(\omega) \\ &= \beta_0(L_2 - L_1) + \beta_1(L_2 - L_1)(\omega - \omega_0). \end{aligned} \quad (10)$$

If $L_2 - L_1$ is sufficiently small, it is possible to minimize the phase ambiguity and estimate the constant term $\beta_0$ and the phase effective index $n_{\text{eff}}$. The accuracy of the estimation increases for larger values of $L_1 - L_2$, and hence, a trade off exists between accuracy and easy phase unwrapping. In this case, the term $\beta_1(L_2 - L_1)$ is small (because of the small difference $L_2 - L_1$) and does not allow an accurate estimation of $\beta_1$. To this purpose, we can write the phase associated to the entire waveguide section of a probe element as

$$\begin{aligned}\varphi_T(\omega) &= \varphi_C(\omega) - \varphi_A(\omega) \\ &= \beta_0(L_1 + L_2) + \beta_1(L_1 + L_2)(\omega - \omega_0). \end{aligned} \quad (11)$$

Taking into account only the linear term of the phase defined in Equation (11), we can now accurately estimate $\beta_1$ (because the term $\beta_1(L_2 + L_1)$ is sufficiently large) and then calculate the group index $n_g$. The accuracy in the estimation of the group index increases for larger values of $L_1 + L_2$.

The waveguide exploited for the experiment is rib-shaped with 1 $\mu$m-thick InGaAsP core on top of the InP substrate, etch depth of 1.7 $\mu$m and no top cladding, as shown in Fig. 6(b). The core of the waveguide is composed by $In_{1-x}Ga_xAs_yP_{1-y}$ with $y = 0.26$, corresponding to a bandgap energy of 1.17 eV at room temperature. The waveguide width is approximately 2.2 $\mu$m and the total length is about 6.3 mm. The PROW is realized on the waveguide by means of ten weak broadband reflectors each one made of a 30 $\mu$m-wide waveguide section with a length equal to the waveguide width. The first crossing occurs at about 150 $\mu$m from the input facet. The distance between the crossings increases with steps of 100 $\mu$m from 156 to 956 $\mu$m. In this particular experimental case we assume the optical properties being constant on the entire waveguide. We can identify a maximum of 8 probe elements. For example, the first probe is realized exploiting the first, second, and third reflective sections; the second probe element consists of the second, third, and fourth crossings and so on. Each probe element is characterized by the same value $L_2 - L_1 = 100\,\mu$m but different total length ($L_1 + L_2$ ranges from 400 $\mu$m of the first probe to 1800 $\mu$m of the last probe element). Since the accuracy of the estimation for the group index improves for longer probe elements, only the last five probes are actually considered during the measurements.

### B. Experimental results

In order to perform the measurements, the sample was placed on a holder equipped with a Peltier element, a thermo-resistance and a feedback loop that stabilize the temperature with an accuracy of 0.1 K. Measurements were performed at temperatures of 300, 305, 310, and 320 K. A tunable laser was used as source with central emitting wavelength of 1.55 $\mu$m and a range of 60 nm. The optical spectrum of the light back-reflected by the PROW was measured with an optical spectrum analyzer. The dependence of phase effective index from the temperature was calculated at each probe with the technique described in Sec. IV A through an incremental estimation. In particular, for the $k-$th probe element the variation of the phase effective index $\Delta n_{\text{eff},k}^{i+1}$ between temperature $T_{i+1}$ and $T_i$ can be calculated as

$$\Delta n_{\text{eff},k}^{i+1} = \left(\Delta\varphi_k^{i+1} - \Delta\varphi_k^{i}\right)\frac{c}{2(L_2 - L_1)\omega_0}. \quad (12)$$

where $\Delta\varphi_k^i$ represents the equivalent phase (as defined in Equation (10)) for the $k-$th probe at the $i-$th temperature. As already discussed, during the experiment $T_i = 300$, 305, 310, and 310 K while $k = 1\ldots8$. The dependence of the group index from the temperature is retrieved for each probe element again with an incremental scheme, but directly by the group index estimation

$$\Delta n_{g,k}^{i+1} = n_g^{i+1} - n_g^{i}. \quad (13)$$

As in the previous case, $n_g^i$ represents the group index measured for the $k-$th probe and the $i-$th temperature. As already discussed, in this case, $k$ ranges from 4 to 8. The difference between the two estimation techniques for the phase and group indices was chosen in order to maximize the accuracy of the measurements.[12] With this approach the expected accuracy for the $n_{\text{eff}}$ and $n_g$ estimation is about $5 \times 10^{-4}$ and $2 \times 10^{-3}$, respectively.

Measurements were performed with both TE and TM polarized modes at the central wavelength $\lambda_0 = 1.55$ $\mu$m. The results of the phase and group indices variations with respect to room temperature (300 K) are reported in Figs. 7(a)–7(d), respectively. Blue dots refer to experimental data (each point is the measurement done on a single probe element of the PROW) while blue lines are a linear fit of the measurements. Error bars report the expected accuracy in both cases. In order to compare the experimental data with the prediction of the method described in Sec. III A, the phase and group indices were simulated for the considered temperature values by means of a mode solver based on the Film-Mode Matching technique.[11] During the simulation, the proposed method was used to calculate the temperature dependence of the refractive index of InP and InGaAsP and the results are reported in Fig. 7 with black lines. The simulated absolute values of the phase and group effective indices for TE mode at 300 K are 3.192 and 3.533, respectively, very close to the indices for TM mode (3.190 and 3.527, respectively). As can be seen, numerical results are in very good agreement with experimental data. In both cases, the

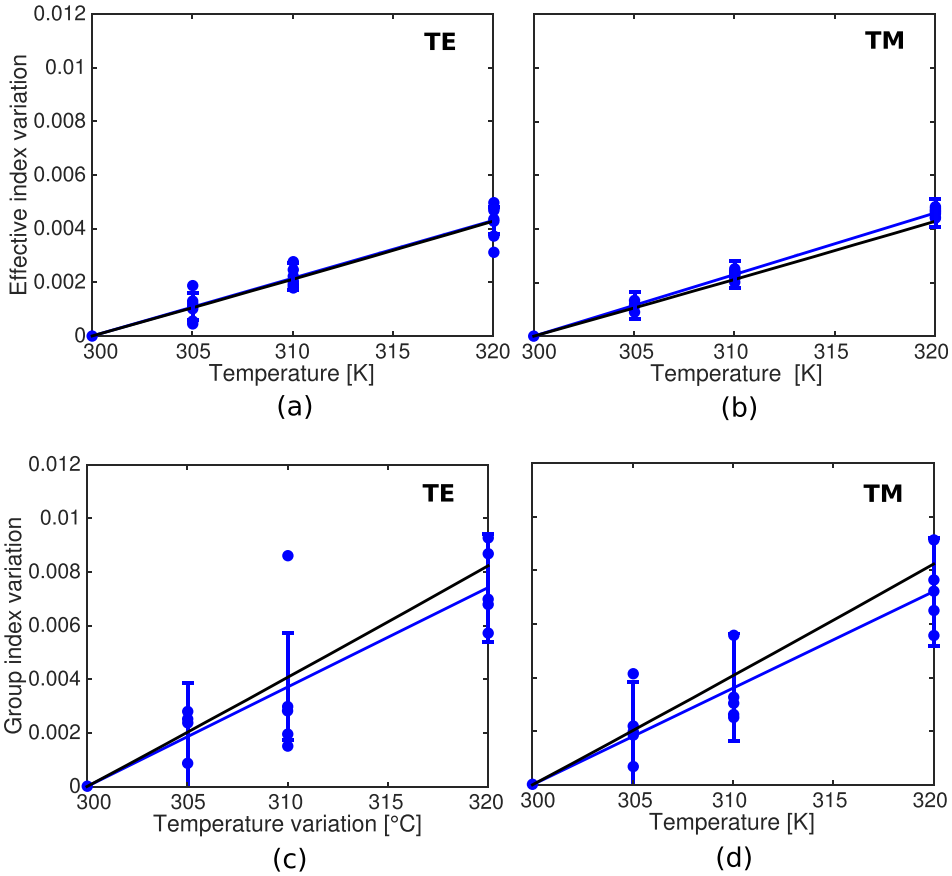


FIG. 7. Variation of effective index and group index with respect to room temperature (300 K) for both (a) and (c) TE and (b) and (d) TM modes. Each point refers to the value measured at a particular probe element (with the expected accuracy represented by the error bars). Blue lines are linear fits done on the experimental data while black lines are the simulations obtained through a mode solver incorporating the method proposed in Sec. III A.

variations of the group index with temperature are larger than the variations of the phase index. Because of the different retrieving techniques, the experimental data for the phase index are much less noisy than the measurement of the group index, in particular, for the TM polarized mode, as can be seen in Fig. 7. In Fig. 7(c) the measured data at temperature variation equal to 310 K are quite noisy and are not considered in the fitting.

Table II reports the thermo-optic coefficients dn/dT calculated from the data reported in Fig. 7 for both experimental data (through the linear fitting, blue lines) and simulations (black lines). As already mentioned, the wavelength dependence is expressed through the thermo-optic coefficients for phase and group effective indices. For the measured values, the ratio between the thermo-optic coefficients of the group index ($dn_g/dT_{TE} = 3.7 \times 10^{-4}$) and phase index ($dn_{\text{eff}}/dT_{TE} = 2.2 \times 10^{-4}$) is 1.68 for TE polarization and slightly smaller (1.57) for TM polarization ($dn_g/dT_{TM} = 3.6 \times 10^{-4}$ and $dn_{\text{eff}}/dT_{TM} = 2.3 \times 10^{-4}$). The values simulated by exploiting the method proposed in Sec. III A are very close to the experimental data for both $n_{\text{eff}}$ and $n_g$. The simulations predict the same thermo-optic coefficients for TE and TM modes. It should be noticed that the difference between TE and TM modes in both phase and group thermo-optic coefficients observed in the experimental data (in the order of $1.5 \times 10^{-5}$) is smaller than the accuracy achievable by the measurement technique.

TABLE II. Measured thermo-optic coefficients $dn_{\text{eff}}/dT$ and $dn_g/dT$ for both TE and TM modes at $\lambda_0 = 1.55$ $\mu$m and comparison with simulated values.

| | TE | TM | Simulation |
|---|---|---|---|
| $dn_{\text{eff}}/dT$ | $2.15 \times 10^{-4}$ | $2.30 \times 10^{-4}$ | $2.16 \times 10^{-4}$ |
| $dn_g/dT$ | $3.74 \times 10^{-4}$ | $3.60 \times 10^{-4}$ | $4.12 \times 10^{-4}$ |

## V. CONCLUSION

In this work, a method to include temperature dependence (along with wavelength and composition dependencies) in the calculation of the refractive index and linear thermo-optic coefficient of $In_{1-x}Ga_xAs_yP_{1-y}$ alloys through the modified single oscillator model was proposed and experimentally validated. The results obtained with the proposed method showed a much better agreement with experimental data available in literature for InP than available methods on different wavelength and temperature ranges. A good agreement with experimental results was shown also in the calculation of the temperature- and wavelength-dependent refractive index of GaAs. The proposed approach was exploited in a Film-Mode Matching solver to calculate the linear thermo-optic coefficients of phase and group effective indices of an InGaAsP-based waveguides. Results are in accordance with experimental data obtained through a reflectometric PROW-based technique, revealing a dependence of the group index on temperature almost twice that of the phase index.

## ACKNOWLEDGMENTS

The authors gratefully acknowledge M. Baier, F. Soares, and N. Grote (Fraunhofer Heinrich Hertz Institut) for the fabrication of the devices.

TABLE III. Comparison between the thermo-optic coefficient of GaAs predicted through the proposed method and experimental data reported in literature.

| Temperature/Wavelength | Data from literature | This work |
|---|---|---|
| 299–359 K, 1.55 $\mu$m | $2.04 \times 10^{-4}$ (Ref. 7) | $1.94 \times 10^{-4}$ |
| 300–450 K, 1.00 $\mu$m | $2.67 \times 10^{-4}$ (Ref. 20) | $2.70 \times 10^{-4}$ |
| 300–600 K, 1.50 $\mu$m | $2.35 \times 10^{-4}$ (Ref. 8) | $2.07 \times 10^{-4}$ |

## APPENDIX: RESULTS FOR GAAS

The method proposed in Sec. III A for the calculation of the refractive index as function of temperature, wavelength, and material composition can be applied also to III-V semiconductors different from $In_{1-x}Ga_xAs_yP_{1-y}$. In order to provide further verification of the reliability of the proposed method, in this appendix, we calculate the refractive index of GaAs in several wavelength and temperature ranges and compare the results with experimental data available in literature.

To this purpose, it is necessary to modify the original Equations (3a)–(3c) in order to properly calculate the characteristics parameters $E_o$, $E_d$, and $E_g$ to be used in the modified single oscillator model (1), (2). As reported in Ref. 19 these parameters for $Ga_{1-x}Al_xAs$ are, at room temperature,

$$E_o(x) = 3.65 + 0.87x + 0.179x^2, \tag{A1a}$$

$$E_d(x) = 36.1 - 2.45x, \tag{A1b}$$

$$E_g(x) = 1.424 + 1.266x + 0.26x^2. \tag{A1c}$$

GaAs is a particular case with $x = 0$ (as InP is a special case of $In_{1-x}Ga_xAs_yP_{1-y}$ with $y = 0$). With the same procedure described in Sec. III A, it is possible to define a temperature-dependent bandgap energy as

$$E_g(T,x) = \left(1.521 - \frac{5.58 \cdot 10^{-4}T^2}{T + 220}\right) + 1.266x + 0.26x^2 \tag{A2}$$

and hence, the equivalent variation of the aluminium concentration

$$\tilde{x} = -2.43 + \sqrt{3.85E_g(T,x) + 0.45} \tag{A3}$$

to be used in Equations (A1a) and (A1b). Table III reports the comparison between the results obtained with the proposed approach for GaAs ($x = 0$) and the experimental data reported in Refs. 7, 8, and 20. As can be seen, as in the case of InP, the predictions agrees with the experiments with a maximum discrepancy in the order of $10^{-5}$.

[1]G. Gilardi, W. Yao, H. R. Haghighi, X. J. M. Leijtens, M. K. Smit, and M. J. Wale, "Deep trenches for thermal crosstalk reduction in InP-based photonic integrated circuits," J. Lightwave Technol. **32**, 4864–4870 (2014).
[2]M. Smit, X. Leijtens, H. Ambrosius, E. Bente, J. van der Tol, B. Smalbrugge, T. de Vries, E.-J. Geluk, J. Bolk, R. van Veldhoven, L. Augustin, P. Thijs, D. DAgostino, H. Rabbani, K. Lawniczuk, S. Stopinski, S. Tahvili, A. Corradi, E. Kleijn, D. Dzibrou, M. Felicetti, E. Bitincka, V. Moskalenko, J. Zhao, R. Santos, G. Gilardi, W. Yao, K. Williams, P. Stabile, P. Kuindersma, J. Pello, S. Bhat, Y. Jiao, D. Heiss, G. Roelkens, M. Wale, P. Firth, F. Soares, N. Grote, M. Schell, H. Debregeas, M. Achouche, J.-L. Gentner, A. Bakker, T. Korthorst, D. Gallagher, A. Dabbs, A. Melloni, F. Morichetti, D. Melati, A. Wonfor, R. Penty, R. Broeke, B. Musk, and D. Robbins, "An introduction to InP-based generic integration technology," Semicond. Sci. Technol. **29**, 083001 (2014).
[3]K. Nakajima, A. Yamaguchi, K. Akita, and T. Kotani, "Composition dependence of the band gaps of $In_{1-x}Ga_xAs_yP_{1-y}$ quaternary solids lattice matched on InP substrates," J. Appl. Phys. **49**, 5944–5950 (1978).
[4]R. Madelon and M. Dore, "Derivative transmission measurements of the temperature dependance of the $\gamma$-$\gamma$ transition in the $Ga_{0.73}In_{0.27}As_{0.59}P_{0.41}$ compound," Solid State Commun. **39**, 639–641 (1981).
[5]J.-P. Weber, "Optimization of the carrier-induced effective index change in InGaAsP waveguides-application to tunable Bragg filters," IEEE J. Quantum Electron. **30**, 1801–1816 (1994).
[6]S. Adachi, "Refractive indices of III–V compounds: Key properties of InGaAsP relevant to device design," J. Appl. Phys. **53**, 5863–5869 (1982).
[7]J. P. Kim and A. M. Sarangan, "Temperature-dependent sellmeier equation for the refractive index of $Al_xGa_{1-x}As$," Opt. Lett. **32**, 536–538 (2007).
[8]F. G. Della Corte, G. Cocorullo, M. Iodice, and I. Rendina, "Temperature dependence of the thermo-optic coefficient of InP, GaAs, and SiC from room temperature to 600 k at the wavelength of 1.5 $\mu$m," Appl. Phys. Lett. **77**, 1614–1616 (2000).
[9]P. Martin, E. M. Skouri, L. Chusseau, C. Alibert, H. Bissessur *et al.*, "Accurate refractive index measurements of doped and undoped InP by a grating coupling technique," Appl. Phys. Lett. **67**, 881–883 (1995).
[10]E. Gini and H. Melchior, "Thermal dependence of the refractive index of InP measured with integrated optical demultiplexer," J. Appl. Phys. **79**, 4335–4337 (1996).
[11]PhoeniX Software, see http://www.phoenixbv.com for Optodesigner.
[12]D. Melati, A. Alippi, and A. Melloni, "Waveguide-based technique for wafer-level measurement of phase and group effective refractive indices," IEEE J. Lightwave Technol. **34**(4), 1293–1299 (2016).
[13]K. Utaka, K. i. Kobayashi, and Y. Suematsu, "Lasing characteristics of 1.5-1.6 $\mu$m GaInAsP/InP integrated twin-guide lasers with first-order distributed Bragg reflectors," IEEE J. Quantum Electron. **17**, 651–658 (1981).
[14]F. Fiedler and A. Schlachetzki, "Optical parameters of InP-based waveguides," Solid-state Electron. **30**, 73–83 (1987).
[15]R. Nahory, M. Pollack, W. Johnston, Jr., and R. Barns, "Band gap versus composition and demonstration of Vegards law for $In_{1-x}Ga_xAs_yP_{1-y}$ lattice matched to InP," Appl. Phys. Lett. **33**, 659–661 (1978).
[16]Y. P. Varshni, "Temperature dependence of the energy gap in semiconductors," Physica **34**, 149–154 (1967).
[17]T. Takagi, "Refractive index of $Ga_{1-x}In_xAs$ prepared by vapor-phase epitaxy," Jpn. J. Appl. Phys., Part 1 **17**, 1813 (1978).
[18]T. Takagi, "Dispersion parameters of the refractive index in III-V compound semiconductors," Jpn. J. Appl. Phys., Part 2 **21**, L167 (1982).
[19]M. A. Afromowitz, "Refractive index of $Ga_{1-x}Al_xAs$," Solid State Commun. **15**, 59–63 (1974).
[20]J. Talghader and J. Smith, "Thermal dependence of the refractive index of GaAs and AlAs measured using semiconductor multilayer optical cavities," Appl. Phys. Lett. **66**, 335–337 (1995).
[21]H. Tanobe, Y. Kondo, Y. Kadota, H. Yasaka, and Y. Yoshikuni, "A temperature insensitive InGaAsP-InP optical filter," IEEE Photonics Technol. Lett. **8**, 1489–1491 (1996).
[22]R. Passy, N. Gisin, J. P. V. der Weid, and H. Gilgen, "Experimental and theoretical investigations of coherent OFDR with semiconductor laser sources," IEEE J. Lightwave Technol. **12**, 1622–1630 (1994).
[23]U. Glombitza and E. Brinkmeyer, "Coherent frequency-domain reflectometry for characterization of single-mode integrated-optical waveguides," IEEE J. Lightwave Technol. **11**, 1377–1384 (1993).